

## ORIGINAL ARTICLE

## A pre-clinical model of resistance to induction therapy in pediatric acute lymphoblastic leukemia

AL Samuels<sup>1,7</sup>, AH Beesley<sup>1,7</sup>, BD Yadv<sup>2,7</sup>, RA Papa<sup>2</sup>, R Sutton<sup>3</sup>, D Anderson<sup>4</sup>, GM Marshall<sup>5</sup>, CH Cole<sup>6</sup>, UR Kees<sup>1</sup> and RB Lock<sup>2</sup>

Relapse and acquired drug resistance in T-cell acute lymphoblastic leukemia (T-ALL) remains a significant clinical problem. This study was designed to establish a preclinical model of resistance to induction therapy in childhood T-ALL to examine the emergence of drug resistance and identify novel therapies. Patient-derived T-ALL xenografts in immune-deficient (non-obese diabetic/severe combined immunodeficient) mice were exposed to a four-drug combination of vincristine, dexamethasone (DEX), L-asparaginase and daunorubicin (VXLD). 'Relapse' xenografts were characterized by responses to drugs, changes in gene expression profiles and Connectivity Map (CMap) prediction of strategies to reverse drug resistance. Two of four xenografts developed *ex vivo* and *in vivo* drug resistance. Both resistant lines showed altered lipid and cholesterol metabolism, yet they had a distinct drug resistance pattern. CMap analyses reinforced these features, identifying the cholesterol pathway inhibitor simvastatin (SVT) as a potential therapy to overcome resistance. Combined *ex vivo* with DEX, SVT was significantly synergistic, yet when administered *in vivo* with VXLD it did not delay leukemia progression. Synergy of SVT with established chemotherapy may depend on higher drug doses than are tolerable in this model. Taken together, we have developed a clinically relevant *in vivo* model of T-ALL suitable to examine the emergence of drug resistance and to identify novel therapies.

Blood Cancer Journal (2014) 4, e232; doi:10.1038/bcj.2014.52; published online 1 August 2014

## INTRODUCTION

Acute lymphoblastic leukemia (ALL) is the most common childhood malignancy, constituting approximately 80% of pediatric leukemia and nearly 30% of all childhood cancers.<sup>1,2</sup> Recent advances in the treatment of pediatric ALL have resulted in increased cure rates to around 85% in the developed world.<sup>3</sup> Better outcome for patients is the result of more intensive combination chemotherapies and improvements in supportive care. These protocols include the administration of multiple chemotherapeutic drugs over a period of at least 2 years.<sup>4</sup> Treatment is comprised of an initial remission-induction therapy (4–5 weeks) followed by intensification or consolidation therapy (~12–26 weeks), re-induction and then maintenance therapy (up to 3 years) to achieve cure.<sup>5</sup> Up to 11 different chemotherapeutic drugs are used, yet it is the response to the agents administered during remission induction therapy that is a major prognostic factor in childhood ALL.<sup>6–8</sup> Typically, they comprise vincristine (VCR), L-asparaginase (ASP), the glucocorticoids dexamethasone (DEX) or prednisone, with or without an anthracycline such as daunorubicin (DNR). Despite the induction treatment resulting in complete remission rates of >95%,<sup>3</sup> up to 20% of pediatric ALL patients relapse and these individuals experience only a 30–50% likelihood of survival.<sup>9</sup> Specifically, although T-cell ALL (T-ALL) represents only 10–15% of all pediatric ALL, it constitutes up to 48% of high-risk patients.<sup>9,10</sup> Moreover, patients who relapse early in the bone marrow (BM; within 18–24 months), as is the case for

the majority of T-ALL relapses, experience a dismal outcome.<sup>9,11</sup> Relapsed ALL is thus a leading cause of cancer-related deaths in children.

Resistance to remission induction drugs, particularly the glucocorticoids, confers poor prognosis in relapsed ALL.<sup>12,13</sup> Understanding the mechanisms underlying development of drug resistance is critical to develop more effective treatment regimens. Pre-clinical models are essential to explore cancer biology, drug resistance mechanisms and to evaluate new drugs. Cell line-derived *in vitro* models are well established for pre-clinical drug development, however, their ability to recapitulate primary disease is limited. In contrast, *in vivo* xenograft models closely resemble their tumor type of origin and more accurately predict the clinical activity of novel compounds in patients, thus the increased use of patient-derived xenografts for pre-clinical modeling.<sup>14</sup> For studying ALL, the non-obese diabetic/severe combined immunodeficient (NOD/SCID) model is well established and allows direct transplantation of leukemia cells from patients.<sup>15,16</sup> Importantly, the phenotype, genotype and kinetics of engraftment into the NOD/SCID mice appear to reflect the human disease with BM infiltration, followed by migration to the spleen, peripheral blood and other hematopoietic organs.<sup>16,17</sup> Moreover, the model demonstrates the clinical relevance of gene expression profiling in ALL.<sup>18</sup> Continuous xenografts can be established by transplanting cells harvested from the spleens of engrafted mice into secondary and tertiary recipient mice, which

<sup>1</sup>Division of Children's Leukaemia and Cancer Research, Telethon Kids Institute, University of Western Australia, Perth, Western Australia, Australia; <sup>2</sup>Leukaemia Biology Program, Children's Cancer Institute, Lowy Cancer Research Centre, University of New South Wales, Sydney, New South Wales, Australia; <sup>3</sup>Molecular Diagnostics, Children's Cancer Institute, Lowy Cancer Research Centre, University of New South Wales, Sydney, New South Wales, Australia; <sup>4</sup>Division of Bioinformatics and Biostatistics, Telethon Kids Institute, University of Western Australia, Perth, Western Australia, Australia; <sup>5</sup>Kids Cancer Centre, Sydney Children's Hospital, Sydney, New South Wales, Australia and <sup>6</sup>School of Paediatrics and Child Health, University of Western Australia, Perth, Western Australia, Australia. Correspondence: Professor RB Lock, Leukaemia Biology Program, Children's Cancer Institute, Lowy Cancer Research Centre, PO Box 81, Sydney, 2031 New South Wales, Australia.  
E-mail: rlock@ccia.unsw.edu.au

<sup>7</sup>These authors contributed equally to this work.

Received 22 May 2014; accepted 17 June 2014

allows the measurement *in vivo* of the effect of drugs or drug combinations, and drug resistance mechanisms.<sup>19,20</sup>

The aim of the current study was to develop a pre-clinical model of induction therapy for pediatric ALL in NOD/SCID mice so that it can be used to study the development of drug resistance *in vivo* and identify alternative therapeutic approaches. We established four T-ALL xenografts from patient samples and mice were treated with an induction-type regimen consisting of VCR, DEX, ASP and DNR (VXLD) in one or more blocks. The resulting outgrowths of two 'relapsed' xenografts were subjected to comprehensive drug testing and gene expression profiling. Using Connectivity Map (CMap) analysis,<sup>20,21</sup> we identified simvastatin (SVT) as a potential resistance-reversing drug, known to inhibit cholesterol synthesis via the mevalonic acid pathway.<sup>22</sup> In this study, we provide proof of concept that the model is suitable to identify alternative therapeutic approaches, and our findings highlight the importance of *in vivo* validation.

## MATERIALS AND METHODS

### Development of T-ALL xenografts and *in vivo* drug treatments

All experimental studies had received prior approval from the Animal Care and Ethics Committee of the University of New South Wales, and the Human Research Ethics Committees of the South Eastern Sydney Local Health District and the University of New South Wales. Samples used in this study were obtained from children treated in Australia and New Zealand Children's Haematology and Oncology Group (ANZCHOG) Study 8 clinical trial ([http://www.anzctr.org.au/trial\\_view.aspx?ID=1568](http://www.anzctr.org.au/trial_view.aspx?ID=1568)), with the exception of sample ALL-29 obtained from a Study 7 patient. Xenograft lines were established from T-ALL diagnosis biopsy samples in the NOD/SCID strain as previously described,<sup>16</sup> and patient demographics are detailed in Table 1. Methods for monitoring engraftment and disease progression, *in vivo* selection of xenograft lines with VXLD and *in vivo* drug efficacy are detailed in the Supplementary Materials and Methods.

### MTT colorimetric assay

Xenograft cells were assessed for single agent and combination *ex vivo* drug sensitivity by MTT assay as detailed in the Supplementary Materials and Methods. The nature of the interaction between drugs (synergy/antagonism) was assessed at each drug concentration using the Bliss additivity model.<sup>23,24</sup>

### Gene expression analysis

Microarray analysis of gene expression using RNA extracted from patient and xenograft cells was carried out as described in the Supplementary Materials and Methods.

## RESULTS

### *In vivo* selection of drug-resistant T-ALL xenograft lines

The xenografts used in this study were derived from diagnosis specimens of T-ALL patients, two of whom relapsed early (< 1 year) and succumbed to their disease (ALL-27 and ALL-31, Table 1). The latter patient was highly refractory to treatment, and a sample obtained on day 103 was used to generate xenograft ALL-31b (Table 1). This presented the opportunity to compare experimentally derived and clinically derived drug-resistant phenotypes.

We previously optimized an induction-type regimen of VCR, DEX and ASP (VXL) for pre-clinical ALL studies in NOD/SCID mice.<sup>25</sup> To improve the clinical relevance of the model in the current study, we included the anthracycline DNR in the VXL backbone. The maximum tolerated dose of DNR in NOD/SCID mice was 2.5 mg/kg administered i.v. once per week (Supplementary Table 1). At this dose and schedule DNR, delayed disease progression by 8.1 days in the previously characterized T-ALL xenograft ALL-16,<sup>17</sup> and when added to the VXL platform (VXLD) extended the progression delay of ALL-31 from 26.4– to 41.0 days (data not

**Table 1.** Patient demographics for T-ALL xenografts

T-ALL xenograft established from biopsy	Age at diagnosis (years)/sex	Disease status at biopsy	WCC at diagnosis (10 <sup>9</sup> )	Initial response to prednisolone	Minimal residual disease day 33/day 79	Length of CR1 (mo)	Current status	Cytogenetics	Immunophenotype
ALL-27	8.7/M	Diagnosis	526.2	PPR	Negative/negative	10	DOD	46, XY [24]	CD45 <sup>+</sup> /HLA-DR <sup>-</sup> /CD19 <sup>-</sup> / 22 <sup>-</sup> /10 <sup>-</sup> /3+cyto/4 <sup>+</sup> /8 <sup>+</sup> /2 <sup>+</sup> / 7 <sup>+</sup> /34 <sup>-</sup> /13 <sup>-</sup>
ALL-29*	4.9/M	Diagnosis	86.2	ND	2 × 10 <sup>-4</sup> /ND	137	CR1	46, XY	CD45 <sup>+</sup> /HLA-DR <sup>-</sup> /CD19 <sup>-</sup> / 3 <sup>-</sup> /2 <sup>+</sup> /4 <sup>+</sup> /7 <sup>+</sup> /8 <sup>+</sup> /22 <sup>-</sup> /10 <sup>-</sup>
ALL-31	10.3/M	Diagnosis	212.2	PPR	M3/5 × 10 <sup>-1</sup>	0 <sup>a</sup>	DOD	46,XY,del(6)(q21),del(11)(q23)[4]/46,XY[14]	HLA-DR <sup>-</sup> /CD19 <sup>-</sup> /10 <sup>-</sup> /2 <sup>+</sup> / 3 <sup>+</sup> /5 <sup>+</sup> /7 <sup>+</sup> /TCRab <sup>+</sup> /Tdt <sup>+</sup>
ALL-31b <sup>a</sup>	10.3/M	Day 103	212.2	PPR	M3/5 × 10 <sup>-1</sup>	0 <sup>a</sup>	DOD	ND	ND
ALL-33	7.4/M	Diagnosis	121.5	PPR	< 1 × 10 <sup>-4</sup> /negative	73	CR1	46,XY,t(11;14)(p13;q32)[11]/46,idem,t(1;8;9)(q32;1;p21;p22)[8]/46,XY[1], FISH with IgH - intact but on chromosome 11	CD19 <sup>-</sup> /HLA-DR <sup>-</sup> /3 <sup>-</sup> /4 <sup>+</sup> /8 <sup>+</sup> / 2 <sup>+</sup> /5 <sup>+</sup> /7 <sup>+</sup> /10 <sup>-</sup> /34 <sup>-</sup>

Abbreviations: CR1, complete remission 1; DOD, died of disease; M3, marrow > 25% blasts at day 33; ND, not determined; PPR, poor prednisolone responder; T-ALL, T-cell acute lymphoblastic leukemia; WCC, white cell count. <sup>a</sup>Patient ALL-29 was treated on ANZCCSG Study 7 as high risk. This protocol did not have the initial 7 days of prednisolone treatment. <sup>b</sup>Patient ALL-31 was refractory to treatment, resulting in a second biopsy at day 103 that was used to derive ALL-31b. This patient died at 5 months after diagnosis without achieving remission. For immunophenotype analysis, the cutoff for positivity was set at 30%.

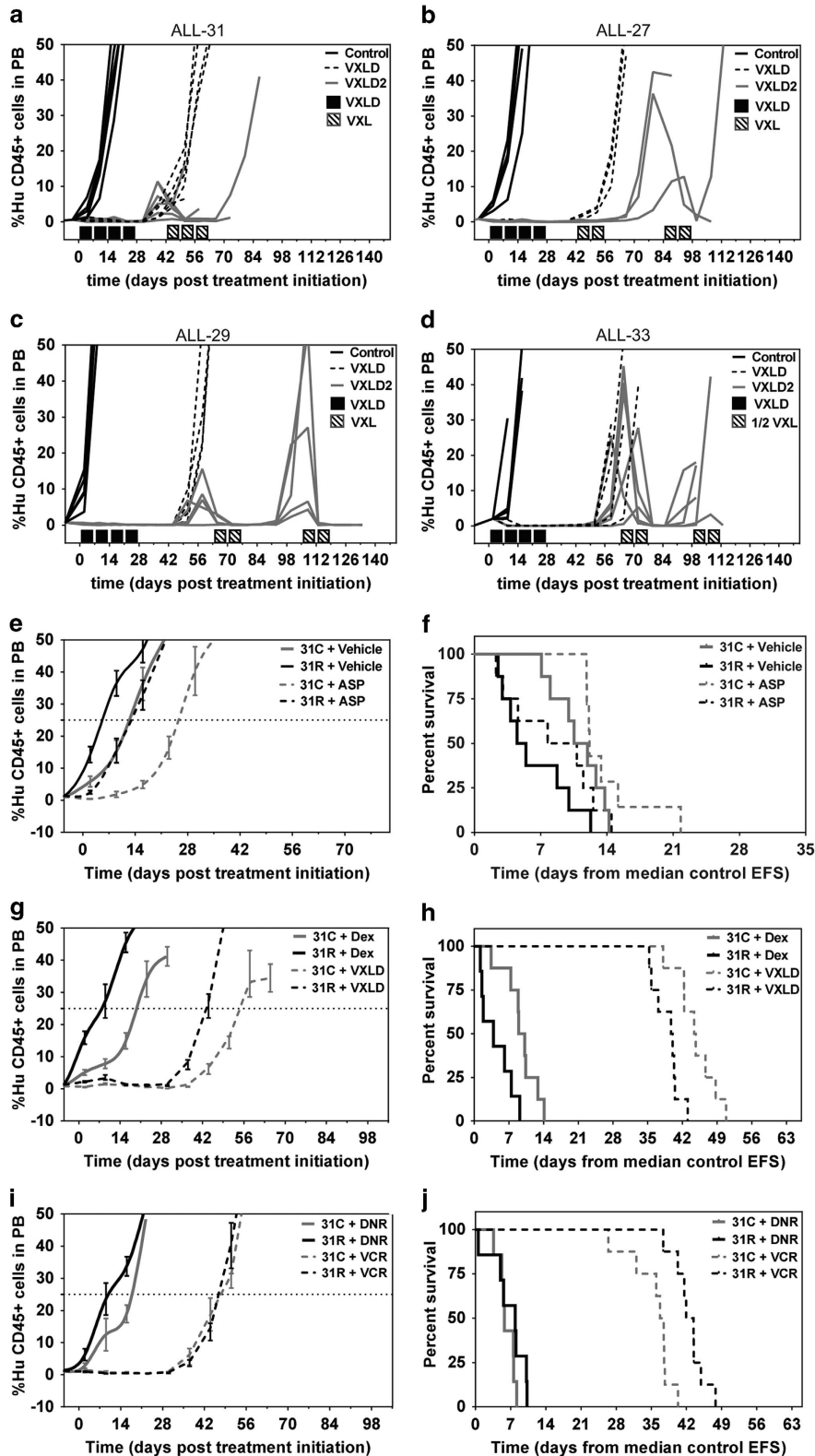
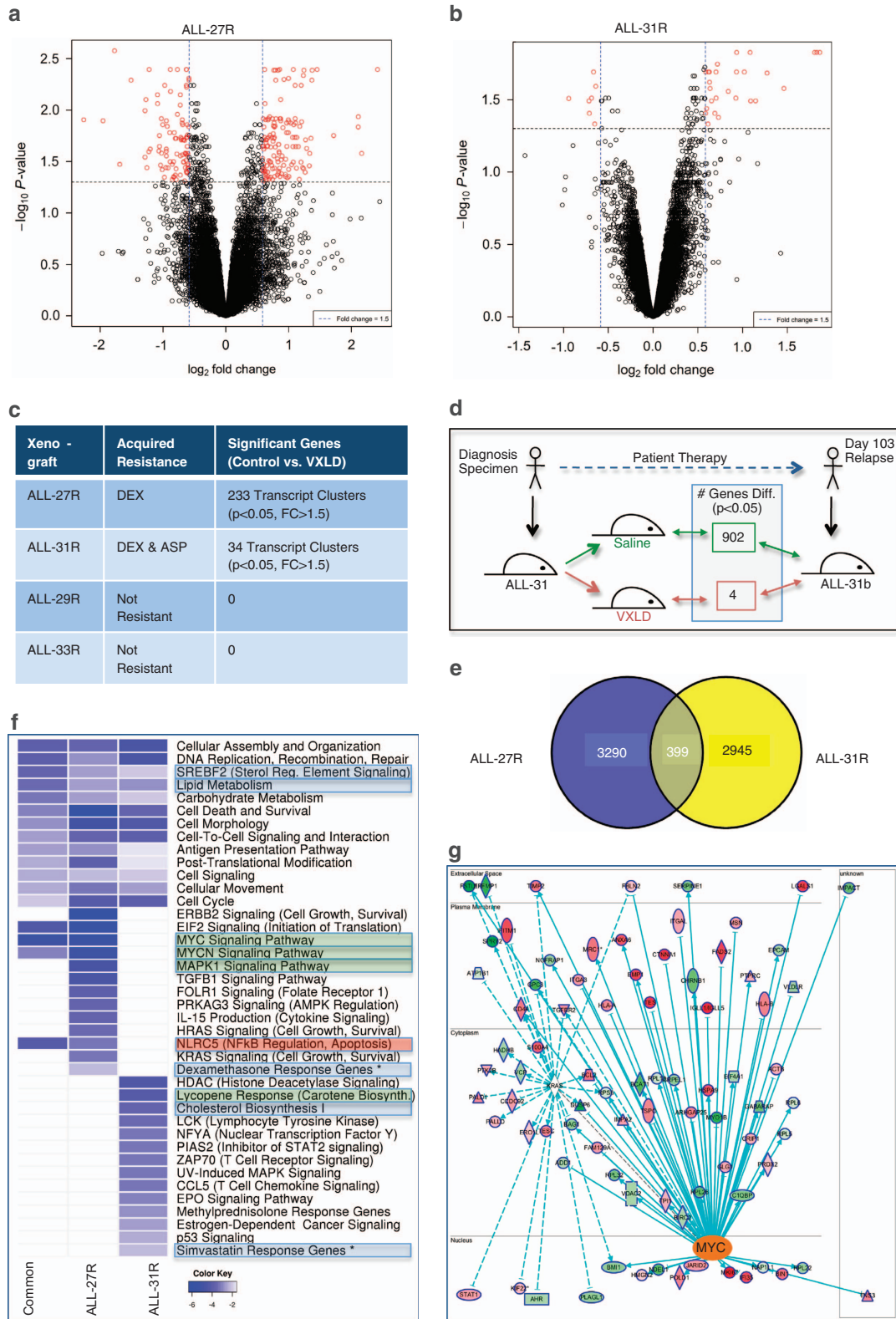


**Figure 1.** *In vivo* drug treatment of T-ALL xenografts. (a) ALL-31, (b) ALL-27, (c) ALL-29 and (d) ALL-33 were treated with either single (VXLD) or multiple (VXLD2) rounds of treatment, or saline (control), to generate lines resistant to multidrug chemotherapy. Acquired drug resistance to single agent ASP (e, f), single agent DNR and VCR (i, j) and single agent DEX, or VXLD combination therapy (g, h) was assessed in ALL-31R (derived from VXLD2-treated ALL-31) and compared with passage-matched ALL-31C, with time course of huCD45<sup>+</sup> cells (e, g, i) and survival plots (f, h, j) for the groups of mice in each drug treatment. Baseline engraftment ALL-31C or ALL-31R treated with saline only is indicated in e.

shown). Therefore, this dose and schedule of DNR exerted anti-leukemic efficacy *in vivo*. We next developed protocols for the *in vivo* selection of drug-resistant xenografts based on the VXLD platform. A 4-week induction schedule was adopted, analogous to

the clinical regimen, which clearly delayed disease progression in all four xenografts (Figures 1a–d). The intention was to allow disease reappearance in the peripheral blood and resume cycles of VXLD treatment until the disease progressed through the





treatment. Based on tolerability and the proportion of mice with re-emergence of disease, we eventually adopted a protocol consisting of a 4-week block of VXLD, followed at disease re-emergence by a 2-week block of half-dose VXL (Figures 1a–d, and Supplementary Table 2). Re-emerging lines (herein labeled 'R') were thus harvested after either one block of therapy ('VXLD') or repeated chemotherapy blocks ('VXLD2'), respectively. Passage-matched controls (labeled 'C') were also harvested for each xenograft line.

#### *Ex vivo* and *in vivo* assessment of drug resistance in relapsing xenografts

Leukemia cells isolated from *in vivo* drug-selected xenografts were tested *ex vivo* against each of the four drugs in VXLD (Supplementary Figure 1). ALL-27R derived from either VXLD or VXLD2 demonstrated increased resistance to DEX, with a trend to higher resistance in the VXLD2 line (Supplementary Figure 1A top panels). Both treatment regimens in ALL-31 were associated with increased resistance to DEX (Supplementary Figure 1A middle panels) and acquired ASP resistance (Supplementary Figure 1A lower panels) compared with the parental line, and again this resistance was more pronounced in ALL-31R derived from the VXLD2 protocol. No acquired resistance to VCR or DNR was observed in ALL-27R and ALL-31R compared with controls (Supplementary Figure 1B). No change in sensitivity to any of the four drugs was observed in ALL-29R and ALL-33R (Supplementary Figure 1C). In summary, DEX and ASP were the main drugs associated with acquired resistance, a phenotype observed in two out of the four xenografts. In each case, the VXLD2 regimen was associated with higher resistance than VXLD, demonstrating the merit of repeated blocks of treatment to establish the model.

To confirm the significance of these *ex vivo* findings, the drug responses of the VXLD2-treated ALL-31R line were compared *in vivo* to ALL-31C (Figures 1e–j). The single-agent dosing regimens are detailed in Supplementary Table 1. ALL-31R itself demonstrated accelerated engraftment in the absence of drug compared with ALL-31C (Figure 1e, vehicle), as well as faster leukemic relapse following the treatment with ASP (Figures 1e and f), DEX or VXLD (Figures 1g and h). *In vivo* resistance to DNR and VCR was not observed (Figures 1i and j). Statistically significant decreases in leukemia progression were observed for DEX (–6.8 days,  $P=0.0112$ ), ASP (–2.9 days,  $P=0.0479$ ) and VXLD (–4.6 days,  $P=0.0026$ ) but not for DNR (1.1 days,  $P=0.57$ ; Supplementary Table 3). Overall, the drug resistance phenotype of ALL-31R observed from *ex vivo* studies was supported by the findings from *in vivo* drug resistance profiling, confirming acquired resistance to both DEX and ASP.

#### Analysis of genes and pathways associated with acquired drug resistance

To identify biological pathways involved in drug resistance and relapse, we performed gene expression profiling of VXLD treated

and controls from each of the xenografts ALL-27, ALL-29, ALL-31 and ALL-33. Volcano plots visually identified transcript clusters with differential gene expression in treated vs control lines, as defined by both adjusted  $P$ -value ( $P < 0.05$ ) and absolute fold change ( $> 1.5$ ). Using this approach, both ALL-27R (Figure 2a) and ALL-31R VXLD-treated cells (Figure 2b) demonstrated significant changes in gene expression, but significant differences were not observed in either ALL-29R or ALL-33R (Figure 2c). This finding appears to be consistent with the known clinical status of the patients from whom xenografts ALL-29 and ALL-33 were generated. Both patients remain in long-term remission and their respective xenografts did not show resistance following treatment with either VXLD or VXLD2. The transcript clusters most significantly associated with acquired resistance in ALL-27R and ALL-31R are detailed in Supplementary Tables 4 and 5.

ALL-31 was derived from the diagnosis specimen of a patient who proved to be refractory to treatment, and a biopsy taken at day 103 was used to generate xenograft ALL-31b (Table 1). An analysis of the gene expression profile of ALL-31b demonstrated it to be remarkably similar to that of the VXLD-treated ALL-31R with only four transcript clusters differentially expressed between the two lines (Figure 2d). In contrast, more than 900 transcript clusters were differentially expressed (adjusted  $P < 0.05$ ) when comparing ALL-31b with the saline-treated ALL-31C (Figure 2d). This indicates that the pre-clinical model of induction therapy that we have developed in this study can effectively recapitulate the development of clinical drug resistance.

To identify biological pathways associated with the development of drug resistance, we compared the wider gene expression changes in ALL-27R and ALL-31R using a less stringent statistical cutoff ( $P < 0.05$  unadjusted) and observed that although there was a distinct overlap (399 transcript clusters with significant change in expression and consistent directionality), a larger proportion of these responses were unique to each line (Figure 2e). Ingenuity Pathway Analysis of the signatures common and unique to ALL-27R and ALL-31R identified some of the apparent mechanisms underpinning these profiles (Figure 2f). Common to both resistant lines were changes to DNA repair pathways, cell death and survival signaling, and cell cycle regulation with obvious relevance for cellular drug sensitivity. Particularly relevant for the DEX-resistant phenotype observed in both ALL-27R and ALL-31R were pathways involved in lipid biosynthesis (Figure 2f, and Supplementary Figure 2), carbohydrate metabolism and *SREBF* signaling (sterol regulator-element binding factor, Supplementary Figure 3). We have previously reported that glucocorticoid resistance in T-ALL is associated with a proliferative metabolism and changes in the cholesterol biosynthesis pathway,<sup>26–28</sup> consistent with the findings from the present study. The acquired DEX-resistance of ALL-27R was also strongly associated with gene networks under the control of MYC, MYCN and MAPK (Figures 2f and g), with the direction of these changes predicted to be consistent with an activated status (a larger version of the network shown in Figure 2g can be found in Supplementary Figure 7). These, together with signatures for

**Figure 2.** Gene expression analysis of acquired drug resistance in T-ALL xenografts. Volcano plots of differential gene expression (VXLD treated vs passage matched control) for (a) ALL-27R and (b) ALL-31R. (c) Correlation between differences in gene expression and drug resistance phenotype for VXLD-treated xenografts. (d) Gene expression comparison of control or VXLD-treated ALL-31R with ALL-31b (derived from the day103 relapse specimen of same patient). (e) Venn diagram showing overlap of resistance-associated gene expression signatures between ALL-27R and ALL-31R (unadjusted  $P < 0.05$  with direction of fold-change taken into account, that is, overlapping genes move in the same direction). (f) Ingenuity Pathway Analysis of resistance-associated gene expression changes affecting ALL-27R and ALL-31R in common (that is, the 399 transcript clusters from Venn diagram intersect) or separately (top 1000 most-significant transcript clusters from either line). Heatmap shows top biological functions, canonical pathways and upstream-network regulators (for example, transcription factors or chemical perturbations) associated with resistance signatures (VXLD-treated vs control). Highlighted pathways are those with a predicted directionality of effect (green, pathway activated in resistant cells; red, pathway downregulated in resistant cells) or networks directly associated with agents used in this study (DEX and SVT, blue highlight). (g) MYC-regulation network associated with acquired resistance in ALL-27R (Ingenuity Pathway Analysis). Colors represent log-fold change (green, expression increased in VXLD-treated xenografts; red, decreased expression in VXLD-treated xenografts; a larger version of this figure can be found in Supplementary Figure 7).

ERBB2 (Supplementary Figure 4), harvey rat sarcoma viral oncogene homolog, kirsten rat sarcoma viral oncogene homolog and transforming growth factor- $\beta$  signaling, indicate the general involvement of pathways involved with cell growth and survival in drug-resistant ALL-27R. A network associated with the cellular response to DEX was also highlighted in this analysis (Figure 2f and Supplementary Figure 5). Resistance in ALL-31R was characterized by pathways associated with cytokine signaling (erythropoietin, chemokine (C-C motif) ligand 5, zeta-chain (TCR) associated protein kinase 70 kDa, LCK proto-oncogene, Src family tyrosine kinase), nuclear signaling (signal transducer and activator of transcription 2, nuclear transcription factor Y, alpha, histone deacetylase), cholesterol biosynthesis and response networks associated with the drug SVT, a blood-cholesterol lowering agent, see Supplementary Figure 6. As part of these latter networks, upregulation of *ASNS* (asparagine synthetase) was evident, a notable observation as ALL-31R demonstrated acquired resistance to ASP, for which *ASNS* upregulation is a known mechanism of resistance.

#### Identification of novel agents to overcome drug resistance

To search for compounds that would be predicted to reverse the resistance phenotypes observed in ALL-27R and ALL-31R, genes significantly associated with acquired resistance (adjusted *P*-value < 0.05) were analyzed using CMap,<sup>21,29</sup> which is an approach we have previously used to identify compounds that have cytotoxic synergy in T-ALL.<sup>26</sup> Compounds with *negative* CMap scores would be predicted to antagonize the drug-resistant phenotype under examination. This analysis identified a large number of potential compounds for each of the xenografts, but there was a high degree of overlap in the classes of drugs identified (Table 2).

Several of these classes (for example, topoisomerase inhibitors, mammalian target of rapamycin inhibitors and histone deacetylase inhibitors) contain agents that are currently being investigated for their benefit in the treatment of ALL.

Of particular interest to us were drug classes with direct relevance for the alteration in lipid and cholesterol metabolism as this was one of the strongest biological features of resistant xenografts (Figure 2f), namely the HMGCR (3-hydroxy-3-methylglutaryl-CoA reductase) inhibitors, peroxisome proliferator-activated receptor  $\gamma$  agonists and inhibitors of fatty acid  $\beta$ -oxidation (Table 2). HMGCR is one of the rate-limiting enzymes for cholesterol synthesis, whereas peroxisome proliferator-activated receptor  $\gamma$  is a nuclear receptor that regulates fatty acid metabolism, cellular energy and apoptosis,<sup>30,31</sup> pathways that have gained a significant amount of interest in recent years as anti-cancer targets.<sup>22,30–38</sup> In addition, transcriptional response to the HMGCR inhibitor SVT was one of the significant networks associated with resistance in ALL-31R (Figure 2f and Supplementary Figure 6). Based on these observations, we selected the HMGCR inhibitor SVT, the peroxisome proliferator-activated receptor  $\gamma$  agonist pioglitazone (PGZ) and the fatty acid  $\beta$ -oxidation inhibitor trimetazidine for further study. We also included the histone deacetylase inhibitor vorinostat (SAHA) as this pathway featured in both the CMap and Ingenuity Pathway analyses (Table 2 and Figure 2f) and we have previously demonstrated the drug to have potential for the reversal of glucocorticoid resistance in pediatric ALL.<sup>39</sup>

As the Broad Institute originally used cell lines exposed to 10  $\mu$ M drug concentrations to generate the CMap, we defined an IC50 value of < 10  $\mu$ M as the cutoff for a drug to exhibit single-agent activity. With the exception of SAHA, none of the novel agents

**Table 2.** Major drug classes predicted by CMap analysis to reverse resistant phenotypes in ALL-27 and ALL-31 VXLD-treated xenografts

Drug class	ALL-27		ALL-31	
	Top compounds	Score	Top compounds	Score
Alkylating drugs	Dacarbazine	-0.74	Lomustine	-0.83
	Cephaeline	-0.57	Cephaeline	-0.79
Antibiotics	Oleandomycin	-0.69	Altretamine	-0.75
	Roxithromycin	-0.68	Ceftazidime	-0.85
	Amoxicillin	-0.68	Sulfamethizole	-0.75
	<b>Vorinostat</b>	-0.33	Meclocycline	-0.74
Histone modifiers (acetylation/demethylation)			<b>Vorinostat</b>	-0.48
			Azacitidine	-0.92
HMGCR inhibitors	<b>Simvastatin</b>	-0.70	<b>Simvastatin</b>	-0.47
Modulators of fatty acid	<b>Trimetazidine</b>	-0.71	<b>Pioglitazone</b>	-0.47
Metabolism (PPAR $\gamma$ agonists/ $\beta$ -oxidation inhibitors)			15 $\delta$ Prostaglandin J2	-0.45
mTOR/PI3K inhibitors	Quinostatin	-0.85	Resveratrol	-0.76
Non-steroidal anti-inflammatory	Flufenamic acid	-0.53	Flufenamic acid	-0.54
Organics (amides/amines/azoles/alkaloids)	Propylthiouracil	-0.85	Naringenin	-0.80
	CP-944629	-0.72	Piperine	-0.78
	Riboflavin	-0.67	Luteolin	-0.72
	Scopolamine	-0.67	Phenoxybenzamine	-0.99
Receptor antagonists (muscarinic/adrenergic)			Diphepanil	-0.79
Steroids	Norethisterone	-0.81	Equilin	-0.83
	Cortisone	-0.71	Bethamethasone	-0.75
	Danazol	-0.68	Prednicarbate	-0.73
	Camptothecin	-0.73	Camptothecin	-0.94
Topoisomerase inhibitors/DNA intercalators	Mitoxantrone	-0.73	Irinotecan	-0.99
			Kaempferol	-0.81
			Daunorubicin	-0.75

Abbreviations: ALL, acute lymphoblastic leukemia; CMap, Connectivity Map; HMGCR, 3-hydroxy-3-methylglutaryl-CoA reductase; mTOR, mammalian target of rapamycin; PI3K, phosphatidylinositol 3-kinase; PPAR $\gamma$ , peroxisome proliferator-activated receptor  $\gamma$ ; VXLD, vincristine, dexamethasone, *L*-asparaginase and daunorubicin. Top compounds in each category are indicated, along with CMap enrichment score; bold entries indicate those compounds selected for further study.

demonstrated potent single-agent *in vitro* efficacy against the parental lines (Supplementary Table 6). The combination of DEX and SVT demonstrated different interaction effects in ALL-27R (Figure 3a) and ALL-31R (Figure 3b), with significant synergy only evident for the latter, consistent with the observation that SVT-response networks and cholesterol metabolism were associated

most strongly in this xenograft. The synergy effect was not significant, however, in the ALL-31C control line (see Figure 3e) indicating that this effect was indeed related to the reversal of a resistant phenotype. Unexpectedly, SAHA was antagonistic with DEX in both ALL-27R and ALL-31R, but the effect was milder in ALL-31R (Figures 3c, d and e). Trimetazidine showed no

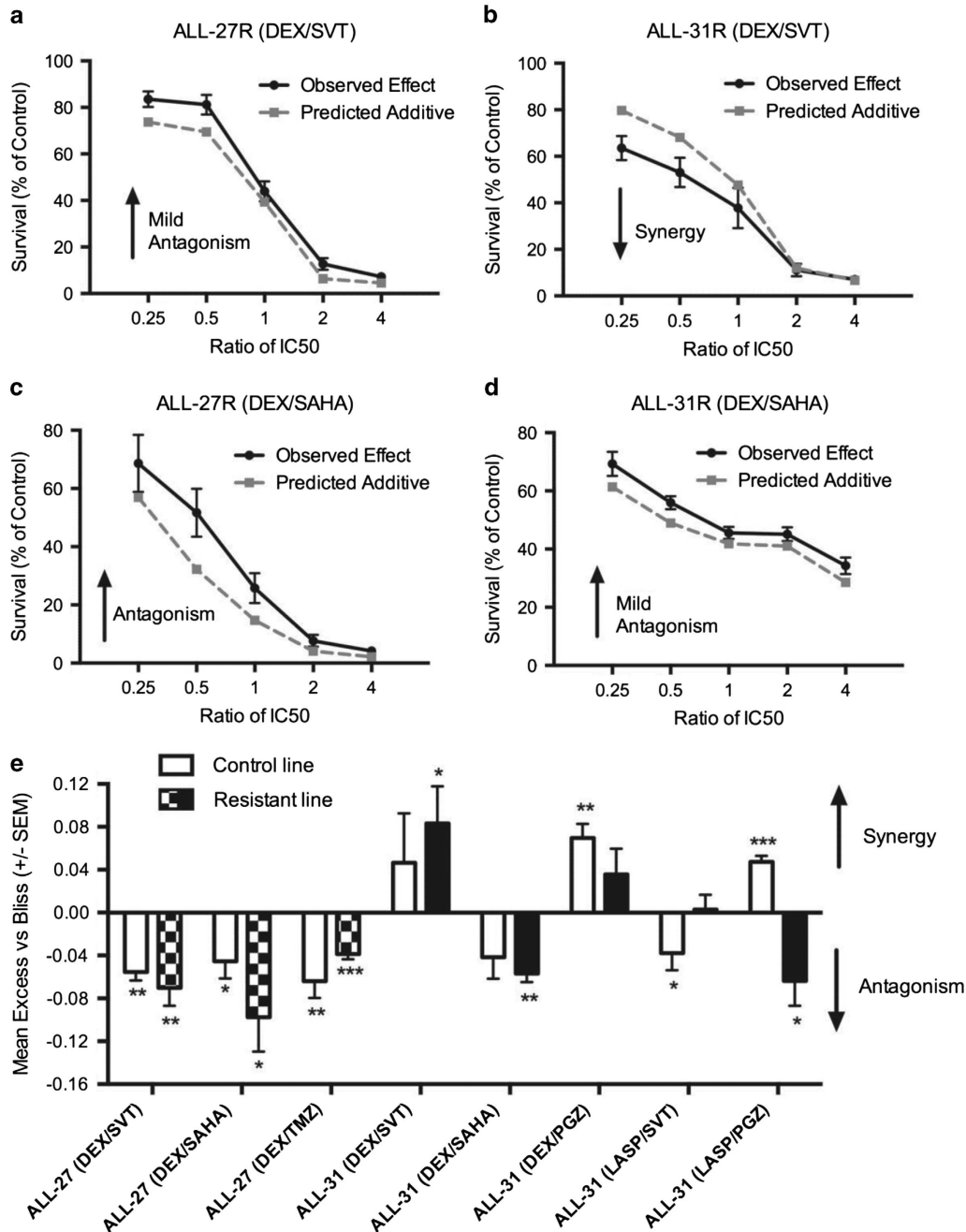


**Figure 3.** *Ex vivo* drug synergy assessment in T-ALL xenograft lines. The cytotoxicity of the indicated drugs in cells from resistant (VXLD2-treated) xenografts was assessed by MTT assay both as single agents and in combination, using fixed IC<sub>50</sub> ratios. A comparison of observed (mean ± s.e.m.) and predicted cytotoxic drug responses is shown for (a) ALL-27R (combined DEX+SVT), (b) ALL-31R (combined DEX+SVT), (c) ALL-27R (combined DEX+SAHA) and (d) ALL-31R (combined DEX+SAHA), with deviations from the predicted curve corresponding to antagonistic (less than additive cytotoxic effects) or synergistic (greater than additive cytotoxicity) effects as indicated. (e) The size of the deviation from Bliss additivity across all IC<sub>50</sub> ratios was averaged across experiments (*n* = 3 to 5 independent experiments per drug combination) to obtain the net synergy effect over all drug concentrations for that combination (± s.e.m.). Positive scores represent a mean cytotoxic effect greater than that predicted by additive effects alone and thus indicate a net synergistic relationship between the two drugs over all drug concentrations tested (*vice versa* for antagonism). Significant positive or negative deviation of the mean from zero was assessed by one-tailed *t*-test, \**P* < 0.05, \*\**P* < 0.01, \*\*\**P* < 0.001.

synergy with DEX in ALL-27C/ALL-27R (Figure 3e; trimetazidine not tested in ALL-31), but PGZ demonstrated synergism with DEX in both ALL-31C and ALL-31R (Figure 3e). Synergy of PGZ was also seen in combination with ASP in ALL-31C, but in ALL-31R, it was associated with antagonism (Figure 3e). In summary, of the combinations tested, only SVT showed significant synergy with DEX in any of the resistant xenografts, that being ALL-31R.

#### *In vivo* efficacy of SVT in the treatment of drug-resistant T-ALL

We next wished to determine whether the apparent benefit of SVT to overcome resistance in ALL-31R could be translated *in vivo*. As the identification of SVT as a therapy from gene expression profiling was derived from experiments based on the VXLD protocol, these *in vivo* studies were designed to test the combination of SVT and VXLD. The maximally tolerated dose for SVT when used in combination with VXLD was 20 mg/kg, and the aim was to determine whether SVT could reverse or delay leukemia relapse induced by a 4-week multidrug induction regimen.

SVT alone induced no significant delay of ALL-31R engraftment to the spleen, BM or peripheral blood (Figures 4a–c), and we observed no *in vivo* synergy of SVT in combination with VXLD, with almost identical patterns of engraftment (Figures 4a–c). SVT as a single agent did not significantly increase mouse event-free survival, whereas VXLD treatment significantly delayed the progression of ALL-31R by 33.4 days compared with vehicle-treated mice (Figures 4d and e). The combination of SVT and VXLD caused no significant delay in leukemia progression compared with VXLD alone. Thus, despite the findings from gene expression, *in vitro* and *ex vivo* experiments, use of SVT *in vivo* at this dose was unable to sensitize leukemia cells to treatment with VXLD.

## DISCUSSION

In this study, we have reported for the first time the development of a powerful pre-clinical *in vivo* model of ALL induction therapy that allows for the investigation of mechanisms of resistance. The data indicate that the model accurately recapitulates the *in vivo* development of resistance as demonstrated by the comparison of

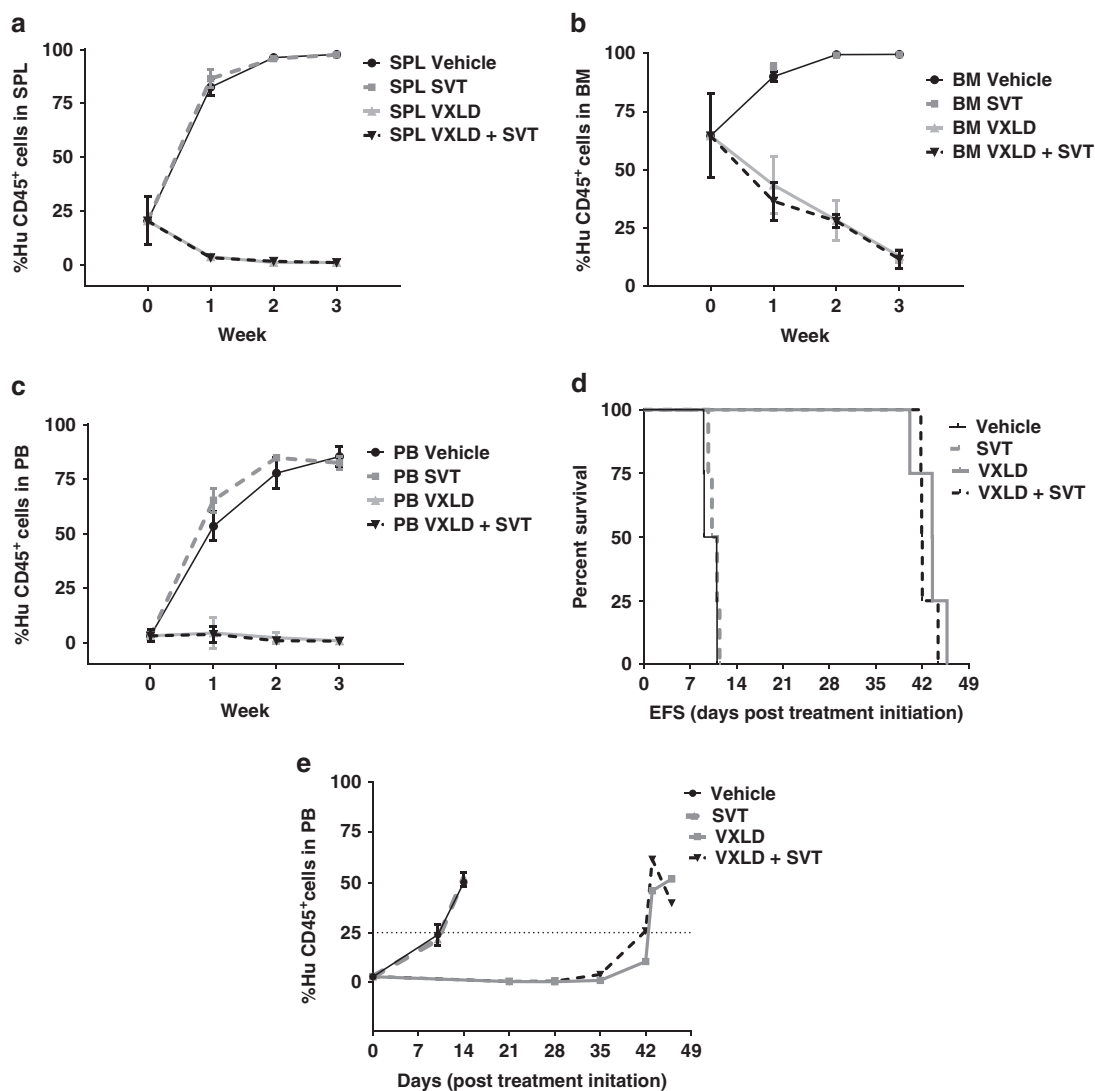


**Figure 4.** Efficacy of SVT (20 mg/kg) for treatment of drug-resistant T-ALL. (a–c) Engraftment of ALL-31R (% Hu CD45<sup>+</sup> cells) over time in (a) spleen, (b) bone marrow or (c) peripheral blood in mice treated with vehicle (black solid line), SVT (gray dotted line), VXLD (gray solid line) or VXLD+SVT (black dotted line). (d, e) Effect of vehicle (black solid line), SVT (gray dotted line), VXLD (gray solid line) and SVT+VXLD (black dotted line) on survival (d) and the time course for the appearance of human CD45<sup>+</sup> cells in peripheral blood (e).



drug-resistant xenografts derived experimentally (ALL-31R) vs clinically (ALL-31b, from a therapy-resistant patient). The differences in gene expression observed between diagnosis and relapse, or parental and drug-treated xenograft lines, may reflect phenotypic changes of the leukemia cells themselves, the selection and out-growth of resistant subpopulations present at the time of diagnosis,<sup>40</sup> or a combination of both mechanisms.<sup>41,42</sup> Under either scenario, the model developed here appears to represent a clinically relevant model of resistance to induction therapy. Using this approach, we have identified biological signatures associated with the development of resistance *in vivo* and have ascertained, as one might expect, that patterns of resistance are different among tumors derived from individual patients. In two of the four leukemia lines tested, no drug resistance emerged after repeated drug treatment, and this correlates with the clinical course of the patients in question as these individuals remain in clinical remission. However, the two other leukemia lines (ALL-27R and ALL-31R) developed drug-resistant phenotypes associated with distinct changes in gene expression, including a prominent activation of MYC and MAPK signaling in one case, and a deregulation of cytokine and nuclear signaling networks in the other. Importantly, changes to lipid and carbohydrate metabolism featured in both resistant lines, an observation that led us to focus on a number of agents that modulate these pathways as a proof-of-concept approach to overcome resistance in ALL.

The inclusion of SVT in ALL therapy regimens is an attractive concept as the drug is generally well tolerated (it is commonly used as an anti-hypercholesterolemia agent) and could potentially alleviate morbidity associated with osteonecrosis, something that affects up to 70% of ALL patients, and for which high levels of cholesterol and treatment with steroids are known risk factors.<sup>43</sup> Although statins have been demonstrated to have anticancer effects, studies of their potential of chemoresistance reversal in ALL have never been reported.<sup>35,44</sup> However, despite the apparent promise of SVT from the gene expression data and its successful assessment *ex vivo*, these findings did not translate *in vivo*.

Our *ex vivo* fixed ratio combination cytotoxicity assays that validated SVT as a potential resistance-reversing drug required continuous exposure to 10–40  $\mu\text{M}$  SVT for 48 h (Figure 3b and Supplementary Table 6). In a recent study carried out in mice administered with 10 mg/kg SVT via oral gavage,<sup>45</sup> the highest achievable plasma concentration (< 3  $\mu\text{M}$ ) was considerably less than the minimum SVT concentration used in our study to achieve synergy. It may not be surprising, therefore, that daily  $\times 5$  dosing of SVT at 20 mg/kg is unable to recapitulate the continuous exposure to 10–40  $\mu\text{M}$  SVT for 48 h used in our assays. Although a number of studies have now successfully recapitulated *in vitro* CMap findings *in vivo*,<sup>21</sup> many published reports stop at the stage of testing their drug-leads *in vitro*.<sup>20,46</sup> Had we not proceeded to test SVT *in vivo*, we too would have concluded a clinical benefit of SVT in combination with VXLD. It is clear that in using CMap for drug repositioning or drug discovery it is very important to carefully assess the appropriateness of the biological context for the model, and to validate any findings *in vivo*.

Recently, Hartwell *et al.*<sup>47</sup> used a completely different approach of a high-throughput screen in a co-culture system and identified the cholesterol lowering drug, Lovostatin, which had a cell-autonomous activity against AML cells. However, an on-target effect of Lovostatin was limited to *ex vivo* analysis because of the expected low concentration to be achieved in BM for their *in vivo* study. Our data using T-ALL cells are complementary, especially in the context of completely different experimental approaches to identify a similar class of drugs. Failure to see an *in vivo* effect of SVT in our own study is likely related to the concentration achievable in the BM *in vivo* within the limits of toxicity, and is thus likely to be a major important factor in the potential translation of this therapeutic approach into the clinic.

It remains possible that a benefit of SVT in combination with DEX as a single agent (as opposed to the more cytotoxic VXLD regimen) could be achievable if this was to be tested *in vivo*, however, the issue of SVT dosing would remain the same. We have not tested PGZ *in vivo* in this study, however, as an alternative modulator of lipid and cholesterol metabolism; it remains a potential candidate for further therapeutic testing in ALL.

The observation that DEX and SAHA were antagonistic in this study is surprising, given that previous studies, including those from our own groups<sup>39</sup> have suggested that this combination may be of benefit in T-ALL. Therefore, these results will require corroboration in a larger number of T-ALL xenografts. In conclusion, this study has resulted in the development of a clinically relevant *in vivo* model of ALL induction therapy that can be used to interrogate mechanisms of drug resistance. We are now extending this study to larger numbers of ALL xenografts to capture a greater diversity of relapsing profiles and identify alternative therapeutic approaches.

## CONFLICT OF INTEREST

The authors declare no conflict of interest.

## ACKNOWLEDGEMENTS

This study was supported by National Health and Medical Research Council Projects Grants ID513765 and ID1011499, and Research Fellowship (RBL). We thank the patients and staff of Sydney Children's Hospital for the provision of ALL biopsies. Children's Cancer Institute Australia for Medical Research is affiliated with the University of New South Wales and the Sydney Children's Hospitals Network.

## AUTHOR CONTRIBUTIONS

ALS, AHB, URK and RBL designed the study; ALS, AHB, BDY, RAP and DA carried out the experiments and analyzed the data; RS, GMM and CHC provided patient biopsies. All authors contributed to the manuscript.

## REFERENCES

- 1 Kaatsch P. Epidemiology of childhood cancer. *Cancer Treat Rev* 2010; **36**: 277–285.
- 2 Lo Nigro L. Biology of childhood acute lymphoblastic leukemia. *J Pediatr Hematol Oncol* 2013; **35**: 245–252.
- 3 Pui CH, Mullighan CG, Evans WE, Relling MV. Pediatric acute lymphoblastic leukemia: where are we going and how do we get there? *Blood* 2012; **120**: 1165–1174.
- 4 Bhadri VA, Trahair TN, Lock RB. Glucocorticoid resistance in paediatric acute lymphoblastic leukaemia. *J Paediatr Child Health* 2012; **48**: 634–640.
- 5 Pui CH, Evans WE. Treatment of acute lymphoblastic leukemia. *N Engl J Med* 2006; **354**: 166–178.
- 6 Dordelmann M, Reiter A, Borkhardt A, Ludwig WD, Gotz N, Viehmann S *et al*. Prednisone response is the strongest predictor of treatment outcome in infant acute lymphoblastic leukemia. *Blood* 1999; **94**: 1209–1217.
- 7 Den Boer ML, Harms DO, Pieters R, Kazemier KM, Gobel U, Korholz D *et al*. Patient stratification based on prednisolone-vincristine-asparaginase resistance profiles in children with acute lymphoblastic leukemia. *J Clin Oncol* 2003; **21**: 3262–3268.
- 8 Kaspers GJ, Veerman AJ, Pieters R, Van Zantwijk CH, Smets LA, Van Wering ER *et al*. *In vitro* cellular drug resistance and prognosis in newly diagnosed childhood acute lymphoblastic leukemia. *Blood* 1997; **90**: 2723–2729.
- 9 Locatelli F, Schrappe M, Bernardo ME, Rutella S. How I treat relapsed childhood acute lymphoblastic leukemia. *Blood* 2012; **120**: 2807–2816.
- 10 Marshall GM, Dalla Pozza L, Sutton R, Ng A, de Groot-Kruseman HA, van der Velden VH *et al*. High-risk childhood acute lymphoblastic leukemia in first remission treated with novel intensive chemotherapy and allogeneic transplantation. *Leukemia* 2013; **27**: 1497–1503.
- 11 Bailey LC, Lange BJ, Rheingold SR, Bunin NJ. Bone-marrow relapse in paediatric acute lymphoblastic leukaemia. *Lancet Oncol* 2008; **9**: 873–883.
- 12 Kaspers GJ, Wijnands JJ, Hartmann R, Huismans L, Loonen AH, Stackelberg A *et al*. Immunophenotypic cell lineage and *in vitro* cellular drug resistance in childhood relapsed acute lymphoblastic leukaemia. *Eur J Cancer* 2005; **41**: 1300–1303.

- 13 Klumper E, Pieters R, Veerman AJ, Huisman DR, Loonen AH, Hahlen K *et al*. *In vitro* cellular drug resistance in children with relapsed/refractory acute lymphoblastic leukemia. *Blood* 1995; **86**: 3861–3868.
- 14 Tentler JJ, Tan AC, Weekes CD, Jimeno A, Leong S, Pitts TM *et al*. Patient-derived tumour xenografts as models for oncology drug development. *Nat Rev Clin Oncol* 2012; **9**: 338–350.
- 15 Macor P, Secco E, Zorzet S, Tripodo C, Celeghini C, Tedesco F. An update on the xenograft and mouse models suitable for investigating new therapeutic compounds for the treatment of B-cell malignancies. *Curr Pharm Des* 2008; **14**: 2023–2039.
- 16 Lock RB, Liem N, Farnsworth ML, Milross CG, Xue C, Tajbakhsh M *et al*. The nonobese diabetic/severe combined immunodeficient (NOD/SCID) mouse model of childhood acute lymphoblastic leukemia reveals intrinsic differences in biologic characteristics at diagnosis and relapse. *Blood* 2002; **99**: 4100–4108.
- 17 Liem NL, Papa RA, Milross CG, Schmid MA, Tajbakhsh M, Choi S *et al*. Characterization of childhood acute lymphoblastic leukemia xenograft models for the preclinical evaluation of new therapies. *Blood* 2004; **103**: 3905–3914.
- 18 Bhadri VA, Cowley MJ, Kaplan W, Trahair TN, Lock RB. Evaluation of the NOD/SCID xenograft model for glucocorticoid-regulated gene expression in childhood B-cell precursor acute lymphoblastic leukemia. *BMC Genomics* 2011; **12**: 565.
- 19 Houghton PJ, Morton CL, Tucker C, Payne D, Favours E, Cole C *et al*. The pediatric preclinical testing program: description of models and early testing results. *Pediatr Blood Cancer* 2007; **49**: 928–940.
- 20 Wei G, Twomey D, Lamb J, Schlis K, Agarwal J, Stam RW *et al*. Gene expression-based chemical genomics identifies rapamycin as a modulator of MCL1 and glucocorticoid resistance. *Cancer Cell* 2006; **10**: 349–351.
- 21 Qu XA, Rajpal DK. Applications of Connectivity Map in drug discovery and development. *Drug Discov Today* 2012; **17**: 1289–1298.
- 22 Wong WW, Dimitroulakos J, Minden MD, Penn LZ. HMG-CoA reductase inhibitors and the malignant cell: the statin family of drugs as triggers of tumor-specific apoptosis. *Leukemia* 2002; **16**: 508–519.
- 23 Borisy AA, Elliott PJ, Hurst NW, Lee MS, Lehar J, Price ER *et al*. Systematic discovery of multicomponent therapeutics. *Proc Natl Acad Sci U S A* 2003; **100**: 7977–7982.
- 24 Winter GE, Rix U, Carlson SM, Gleixner KV, Grebien F, Gridling M *et al*. Systems-pharmacology dissection of a drug synergy in imatinib-resistant CML. *Nat Chem Biol* 2013; **8**: 905–912.
- 25 Szymanska B, Wilczynska-Kalak U, Kang MH, Liem NL, Carol H, Boehm I *et al*. Pharmacokinetic modeling of an induction regimen for *in vivo* combined testing of novel drugs against pediatric acute lymphoblastic leukemia xenografts. *PLoS ONE* 2012; **7**: e33894.
- 26 Beesley AH, Firth MJ, Ford J, Weller RE, Freitas JR, Perera KU *et al*. Glucocorticoid resistance in T-lineage acute lymphoblastic leukaemia is associated with a proliferative metabolism. *Br J Cancer* 2009; **100**: 1926–1936.
- 27 Beesley AH, Rampellini JL, Palmer ML, Heng JY, Samuels AL, Firth MJ *et al*. Influence of wild-type MLL on glucocorticoid sensitivity and response to DNA-damage in pediatric acute lymphoblastic leukemia. *Mol Cancer* 2010; **9**: 284.
- 28 Beesley AH, Firth MJ, Anderson D, Samuels AL, Ford J, Kees UR. Drug-gene modeling in pediatric T-cell acute lymphoblastic leukemia highlights importance of 6-mercaptopurine for outcome. *Cancer Res* 2013; **73**: 2749–2759.
- 29 Lamb J, Crawford ED, Peck D, Modell JW, Blat IC, Wrobel MJ *et al*. The Connectivity Map: using gene-expression signatures to connect small molecules, genes, and disease. *Science* 2006; **313**: 1929–1935.
- 30 Konopleva M, Andreeff M. Role of peroxisome proliferator-activated receptor-gamma in hematologic malignancies. *Curr Opin Hematol* 2002; **9**: 294–302.
- 31 Koeffler HP. Peroxisome proliferator-activated receptor gamma and cancers. *Clin Cancer Res* 2003; **9**: 1–9.
- 32 Hindler K, Cleeland CS, Rivera E, Collard CD. The role of statins in cancer therapy. *Oncologist* 2006; **11**: 306–315.
- 33 Andela VB, Pirri M, Schwarz EM, Puzas EJ, O'Keefe RJ, Rosenblatt JD *et al*. The mevalonate synthesis pathway as a therapeutic target in cancer. *Clin Orthop Relat Res* 2003; **S59**–S66.
- 34 Infante E, Heasman SJ, Ridley AJ. Statins inhibit T-acute lymphoblastic leukemia cell adhesion and migration through Rap1b. *J Leukocyte Biol* 2011; **89**: 577–586.
- 35 Li HY, Appelbaum FR, Willman CL, Zager RA, Banker DE. Cholesterol-modulating agents kill acute myeloid leukemia cells and sensitize them to therapeutics by blocking adaptive cholesterol responses. *Blood* 2003; **101**: 3628–3634.
- 36 Calabro A, Tai J, Allen SL, Budman DR. *In-vitro* synergism of m-TOR inhibitors, statins, and classical chemotherapy: potential implications in acute leukemia. *Anticancer Drugs* 2008; **19**: 705–712.
- 37 Andela VB, Altuwajiri S, Wood J, Rosier RN. Inhibition of beta-oxidative respiration is a therapeutic window associated with the cancer chemo-preventive activity of PPARgamma agonists. *FEBS Lett* 2005; **579**: 1765–1769.
- 38 Samudio I, Harmaney R, Fiegl M, Kantarjian H, Konopleva M, Korchin B *et al*. Pharmacologic inhibition of fatty acid oxidation sensitizes human leukemia cells to apoptosis induction. *J Clin Invest* 2010; **120**: 142–156.
- 39 Bachmann PS, Piazza RG, Janes ME, Wong NC, Davies C, Mogavero A *et al*. Epigenetic silencing of BIM in glucocorticoid poor-responsive pediatric acute lymphoblastic leukemia, and its reversal by histone deacetylase inhibition. *Blood* 2010; **116**: 3013–3022.
- 40 Anderson K, Lutz C, van Delft FW, Bateman CM, Guo Y, Colman SM *et al*. Genetic variegation of clonal architecture and propagating cells in leukaemia. *Nature* 2011; **469**: 356–361.
- 41 Clappier E, Gerby B, Sigaux F, Delord M, Touzri F, Hernandez L *et al*. Clonal selection in xenografted human T cell acute lymphoblastic leukemia recapitulates gain of malignancy at relapse. *J Exp Med* 2011; **208**: 653–661.
- 42 Choi S, Henderson MJ, Kwan E, Beesley AH, Sutton R, Bahar AY *et al*. Relapse in children with acute lymphoblastic leukemia involving selection of a preexisting drug-resistant subclone. *Blood* 2007; **110**: 632–639.
- 43 Kawedia JD, Kaste SC, Pei D, Panetta JC, Cai X, Cheng C *et al*. Pharmacokinetic, pharmacodynamic, and pharmacogenetic determinants of osteonecrosis in children with acute lymphoblastic leukemia. *Blood* 2011; **117**: 2340–2347.
- 44 Chan KKW, Oza AM, Siu LL. The statins as anticancer agents. *Clin Cancer Res* 2003; **9**: 10–19.
- 45 van de Steeg E, Kleemann R, Jansen HT, van Duyvenvoorde W, Offerman EH, Wortelboer HM *et al*. Combined analysis of pharmacokinetic and efficacy data of preclinical studies with statins markedly improves translation of drug efficacy to human trials. *J Pharmacol Exp Ther* 2013; **347**: 635–644.
- 46 Sanda T, Li X, Gutierrez A, Ahn Y, Neuberger DS, O'Neil J *et al*. Interconnecting molecular pathways in the pathogenesis and drug sensitivity of T-cell acute lymphoblastic leukemia. *Blood* 2010; **115**: 1735–1745.
- 47 Hartwell KA, Miller PG, Mukherjee S, Kahn AR, Stewart AL, Logan DJ *et al*. Niche-based screening identifies small-molecule inhibitors of leukemia stem cells. *Nat Chem Biol* 2013; **9**: 840–848.



This work is licensed under a Creative Commons Attribution-NonCommercial-NoDerivs 4.0 International License. The images or other third party material in this article are included in the article's Creative Commons license, unless indicated otherwise in the credit line; if the material is not included under the Creative Commons license, users will need to obtain permission from the license holder to reproduce the material. To view a copy of this license, visit <http://creativecommons.org/licenses/by-nc-nd/4.0/>

Supplementary Information accompanies this paper on Blood Cancer Journal website (<http://www.nature.com/bcj>)